chemistry

MDPI

Article

Yb to Tb Cooperative Upconversion in Supramolecularly Assembled Complexes in a Solution

Lohona K. Soro [1], Cyrille Charpentier [1], Frédéric Przybilla [2], Yves Mély [2], Aline M. Nonat [1] and Loïc J. Charbonnière [1,*]

[1] Equipe de Synthèse Pour l'Analyse (SynPA), Institut Pluridisciplinaire Hubert Curien (IPHC), UMR 7178, CNRS/Université de Strasbourg, 25 rue Becquerel, 67087 Strasbourg, France; lohona.soro@etu.unistra.fr (L.K.S.); charpentierc@unistra.fr (C.C.); aline.nonat@unistra.fr (A.M.N.)

[2] Laboratoire de Bioimagerie et Pathologies, CNRS UMR 7021, Faculté de pharmacie, Université de Strasbourg, 74 route du Rhin, 67401 Illkirch, France; frederic.przybilla@unistra.fr (F.P.); yves.mely@unistra.fr (Y.M.)

* Correspondence: l.charbonn@unistra.fr

Abstract: The podand-type ligand L, based on a tertiary amine substituted by three pyridyl-6-phosphonic acid functions, forms hydrated complexes with Ln^{3+} cations. The luminescence properties of the YbL complex were studied in D_2O as a function of the pD and temperature. In basic conditions, increases in the luminescence quantum yield and the excited state lifetime of the Yb centered emission associated with the $^2F_{5/2} \rightarrow {}^2F_{7/2}$ transition were observed and attributed to a change in the hydration number from two water molecules in the first coordination sphere of Yb at acidic pH to a single one in basic conditions. Upon the addition of $TbCl_3$ salts to a solution containing the YbL complex in D_2O, heteropolynuclear Yb/Tb species formed, and excitation of the Yb at 980 nm resulted in the observation of the typical visible emission of Tb as a result of a cooperative upconversion (UC) photosensitization process. The UC was further evidenced by the quadratic dependence of the UC emission as a function of the laser power density.

Keywords: lanthanides; luminescence; upconversion; supramolecular chemistry; cooperative sensitization

Citation: Soro, L.K.; Charpentier, C.; Przybilla, F.; Mély, Y.; Nonat, A.M.; Charbonnière, L.J. Yb to Tb Cooperative Upconversion in Supramolecularly Assembled Complexes in a Solution. *Chemistry* **2021**, *3*, 1037–1046. https://doi.org/10.3390/chemistry3030074

Academic Editor: Nobuo Kimizuka

Received: 30 July 2021
Accepted: 1 September 2021
Published: 6 September 2021

1. Introduction

The upconversion (UC) phenomenon is an anti-Stokes process in which low-energy photons are converted into higher energy ones. This generally results in the observation of visible-to-NIR emission upon excitation in the NIR domain [1,2]. This process is particularly useful for applications in biology, as the excitation and emission wavelengths match the biological window where the background is low. It thus provides a low autofluorescence background and a high penetration depth [3–5].

Although it is mostly observed in the solid state [6–8], examples at the molecular scale in solutions [9–12] are flourishing thanks to the wide use of lanthanides, with their unique luminescence properties such as long luminescent lifetimes and line-like emission spectra [13,14]. The molecular strategy opens the door to new perspectives in biological applications, considering that it might resolve the drawbacks due to the biotoxicity and hazardous reproducibility of nanomaterials [15].

However, in contrast to solid state devices and nanoparticles [7], the design of the molecular devices in solution is still challenging as a result of important non-radiative deactivations due to energy transfer to OH, NH and CH oscillators [16,17]. These oscillators favor the decay of the intermediate excited state and inhibit the absorption of a second photon or of an energy quantum that is mandatory to reach and emit at a higher energy. One can limit these deactivations by (1) using deuterated oscillators as in D_2O which have less impact on quenching of the intermediate state [18]; (2) protecting the cation with a polydentate ligand, thereby limiting the presence of the solvent in the first coordination

sphere [19]; and (3) introducing bulky substituents which will keep the solvent molecules away from the NIR emitters [20]. Thanks to these strategies, the number of reported molecular upconverting devices has increased in the last decade.

Among the different mechanisms used to develop upconverting devices [1,21], ETU is reported to be the most efficient for the observation of UC at the molecular scale [22]. Its efficiency results from the possibility of having at least one sensitizer transferring its energy to an emitting acceptor center. Thanks to its unique $^2F_{5/2} \rightarrow {}^2F_{7/2}$ electronic transition at 980 nm, Yb(III) is the most common sensitizer used, and it allows for reaching the excited state of numerous other lanthanides such as Eu, Tb, Ho, Er or Tm, all of which can emit in the visible spectrum [11,23–25]. Between those different pairs, the Yb/Tb one introduces a particular mechanism called cooperative sensitization [11,12,26,27]. This mechanism helps to overstep the absence of resonant electronic transition between Yb and Tb, but the efficiency is expected to be weak. In that case, the UC process is possible by exciting 2 Yb centers, which then transfer their energy to the excited state of the Tb ($^5D_4$), allowing its emission in the visible spectrum (Scheme 1).

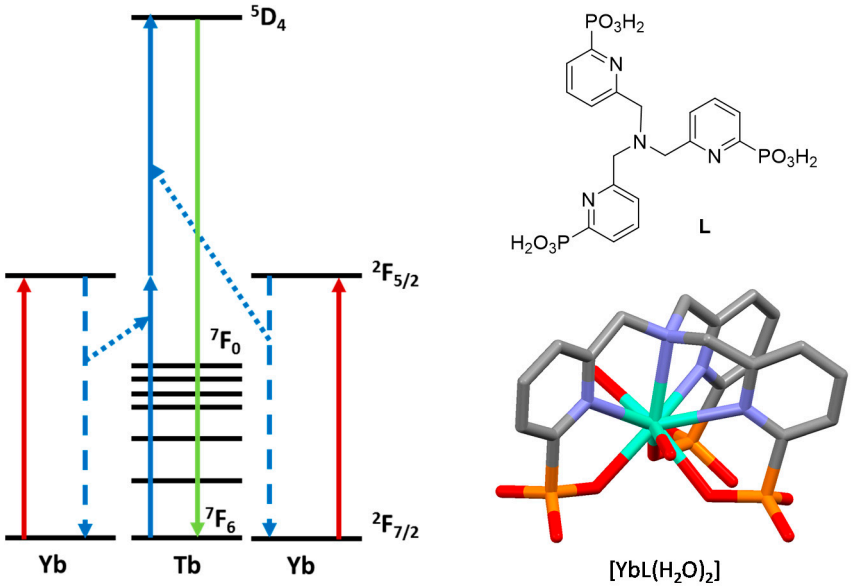

Scheme 1. (**left**) Principle of the cooperative sensitization between Yb and Tb [27]. (**right**) Representation of ligand L and its dihydrated Yb complex (H atoms are omitted for clarity).

Considering our previous findings on the cooperative sensitization of Tb by Yb complexes [11,12], we anticipated that a Yb complex formed by complexation with the heptadentate ligand L (Scheme 1) [28] might offer opportunities to observe UC in D_2O solutions. The spectroscopic properties of the YbL complex were studied in detail together with the interactions of the complex with Tb cations and were shown to allow the formation of heteropolynuclear Yb/Tb complexes that exhibit UC in D_2O.

2. Materials and Methods

The (YbL) complex was prepared by following a previously described procedure [28]. Spectroscopic measurements were performed with 10 × 10 mm^2 quartz suprasil certified cells (Helma Analytics). The steady state emission spectra were recorded on an Edinburgh Instrument FLP920 spectrometer working with a continuous 450-W Xe Lamp and a red-sensitive R928 photomultiplier from Hamamatsu in a Peltier housing for visible detection (230–900 nm) or a Hamamatsu R5 509-72 photomultiplier for the Vis-NIR part. 330-nm and 850-nm high-pass filters were used to eliminate the second-order artifacts when recording in the visible and NIR spectra, respectively. The steady state upconversion emission spectra were recorded on the FLP920 spectrometer using an MDL-3 III-980-nm 2-W laser (CNI Laser) with a 850-nm high-pass filter between the source and the sample to remove

any potential visible excitation. The spectra were recorded using the Peltier-cooled R928 photomultiplier from Hamamatsu, using a fully opened emission slit width (20 nm) by accumulation of 10 spectra at 1 point/nm, with a dwell time of 0.1 s per nm. The pD value was adjusted with a solution of NaOD and a solution of DCl and was calculated with use of the equation of Mikkelsen (pD = pH + 0.4) [29].

The phosphorescence lifetimes were measured with the same instrument working in the multi-channel spectroscopy mode and using a Xenon flash lamp as the excitation source. Errors for the luminescence lifetimes were estimated to be ±10%.

The upconversion quantum yields were measured by following the published procedures [6,11] with a diluted solution (optical density < 0.05) using [TbGlu(H_2O)]Na as a reference [30].

Low-temperature measurements were performed with a Mercury iTC thermocryostat equipped with a HiCUBE turbopump. The solution was prepared with 10% glycerol in a Tris buffer (10 mM, pH 7).

Power-dependent steady state and time-resolved UC luminescence measurements were performed in quartz cuvettes (Hellma QS Semi-Micro Cells). The continuous-wave laser beam (λ = 975 nm) of a single-mode fiber-coupled laser diode was collimated (Thorlabs, TC12APC-980, Ottawa, Canada) and focused in the cuvette by a +100-mm focal length lens. From the measured beam waist radius (w = 30.6 μm), we estimated the average excitation intensity in the beam waist to be 8.1 kW/cm^2 at the maximum laser power. The emission of the sample was collected by a 10 × 0.25 numerical aperture objective and focused on an avalanche photodiode (Excelitas, SPCM-AQRH-16, Wiesbaden, germany). The scattered laser light was removed by a low-pass filter (Chroma, ET750-SP-2P, Olching, Germany) and a band-pass filter (Semrock, FF01-550/88-25, Vanves, France). For the steady state measurements (emitted intensity as a function of the excitation intensity), the output power of the laser was adjusted electronically (by varying the current intensity sent to the diode) and optically by using neutral density filters (Thorlabs) and then systematically measured by a power meter (Newport, 1917R and Ophir, 30A-BB-18). The signal of the photodiode was collected by a computer equipped with a multifunction input/output card (National Instruments multifunction board, PCIe 6711). During the time-resolved measurements, the laser output was modulated electronically at 32 Hz with a 12% duty cycle square waveform by a multifunction input/output card (National Instruments multifunction board, PCIe 6361). The single-photon events detected by the photodiode and the synchronization signal of the laser were recorded by a time-correlated single-photon counting board (Becker & Hickl, SPC-830, Berlin, Germany). SPCM 9.75 software (Becker & Hickl) was used to both record the data and build the photon distribution over time. Experimental luminescence decays were fitted by using the coupled differential rate equations model discussed in the main text in Matlab 2017b.

3. Results and Discussions

3.1. Spectroscopic Properties of the YbL Complex

The YbL complex was prepared as previously described [28]. Considering the peculiar hydration change observed for the parent Gd complex [31], the spectroscopic properties of the Yb analog were first studied as a function of the pD in the D_2O solution. Figure 1 shows the evolution of the emission spectra and of the excited state lifetime of the YbL complex at various pD values. When moving from acidic conditions to basic conditions, an increase in the Yb intensity and lifetime was observed. This phenomenon can be explained by a change in the hydration state of the complex as a function of the acidity of the medium. At pD values below six, the complex contained two water molecules in the first coordination sphere, which was completed by the coordination of the heptadentate ligand, forming the [(YbL)(H_2O)$_2$] species. Above a pD of six, deprotonation of one of the phosphonate functions resulted in the hydrogen bridging of two phosphonate functions with a concomitant overall contraction of the ligand around the Ln atom, resulting in the repulsion of one of the two water molecules and the formation of the [(YbL)(H_2O)] species.

Due to the strong quenching effect of water [16,17], the displacement of one water molecule led to a large increase in the luminescence intensity and lifetime. In addition to the main transition observed at 975 nm at a low pD, a hypsochromic shift of the main band toward 970 nm was observed, as well as new bands appearing at ca. 1000 nm and 1040 nm when increasing the pD, together with a shoulder on the high energy tail at ca. 960 nm. While the former bands were ascribed to the $^2F_{5/2} \rightarrow {}^2F_{7/2}$ transitions of Yb with M_J splitting of the ground and excited states [32], the latter was ascribed to hot bands of Yb, as evidenced by the variable temperature measurements (see below) [33].

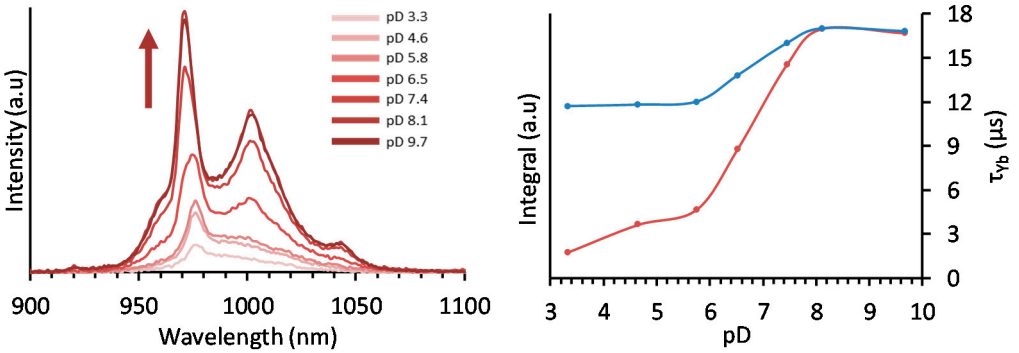

Figure 1. (**left**) Emission spectra of the YbL complex with an increase in the pD value in the D_2O. The arrow indicates the increase of the pD. (**right**) Evolution of the emission integral (red) and the lifetime (blue) (YbL = 9.5 × 10^{-5} M, D_2O), where λ_{exc} = 270 nm.

3.2. Determination of the Yb-Centered Quantum Yield

In order to obtain more insights into the photophysical properties of the Yb complex, the intrinsic luminescence quantum yield of YbL in D_2O was determined using Equation (1). τ_{obs} corresponds to the observed excited state lifetime measured upon excitation of the ligand, and it amounts to 16.7 µs. τ_{rad} is the radiative lifetime of Yb in the complex, which could be determined using the modified Einstein Equation (2) [34–36]. In this second equation, N_A is Avogadro's number, c is the speed of light in a vacuum (in cm s^{-1}), $\tilde{v}$ is the barycenter of the transition in cm^{-1}, n is the refractive index of the medium (n_{D_2O} = 1.33), $\varepsilon(\tilde{v})$ is the absorption spectrum of the transition (in M^{-1} cm^{-1}) and g_l and g_u are related to the degeneracies of the ground and excited states, respectively, and are equal to $2J + 1$, where $J = 7/2$ for g_l and $J = 5/2$ for g_u. A value of 1.13 ms was calculated for τ_{rad}, which is generally between 0.5 and 1.3 ms in the solution [21,37]. Thus, an intrinsic Yb quantum yield of 1.5% could be calculated at a pD of 7.5:

$$\Phi_{Yb}^{Yb} = \frac{k_{rad}}{k_{obs}} = \frac{\tau_{obs}}{\tau_{rad}} \quad (1)$$

$$\frac{1}{\tau_{rad}} = 2303 * \frac{8\pi c n^2 \tilde{\upsilon}^2}{N_A} \frac{g_l}{g_u} \int \varepsilon\left(\tilde{\upsilon}\right) d\tilde{\upsilon}$$
$$\text{With } \tilde{\upsilon} = \frac{\int \tilde{\upsilon} \times \varepsilon\left(\tilde{\upsilon}\right) d\tilde{\upsilon}}{\int \varepsilon\left(\tilde{\upsilon}\right) d\tilde{\upsilon}} \quad (2)$$

The efficiency of sensitization η_{sens} was also determined using Equation (3) [36]. ϕ_L^{Yb} is the luminescent quantum yield upon ligand excitation, and it was equal to 1.2% [28]. Compared with other complexes [38,39], the value of 0.8 obtained for η_{sens} in YbL was higher and pointed to a remarkable transfer from the ligand triplet state to the Yb center:

$$\eta_{sens} = \frac{\phi_L^{Yb}}{\phi_{Yb}^{Yb}} \quad (3)$$

3.3. Low Temperature Measurements

To further characterize this complex, the Yb emission was monitored as a function of the temperature by excitation of the ligand to observe the evolution of the Yb signal in the 77–300 K range in D_2O containing 12% glycerol. As shown in Figure 2, three sharp bands were observed, which could be ascribed to the $^2F_{5/2} \rightarrow {}^2F_{7/2}$ transitions of Yb with M_J splitting of the ground and excited states [32]. The lifetime was also measured (Table 1), showing a gradual decrease upon heating. The higher lifetime values at a low temperature can be explained by the minimization of the non-radiative transitions due to the solvent.

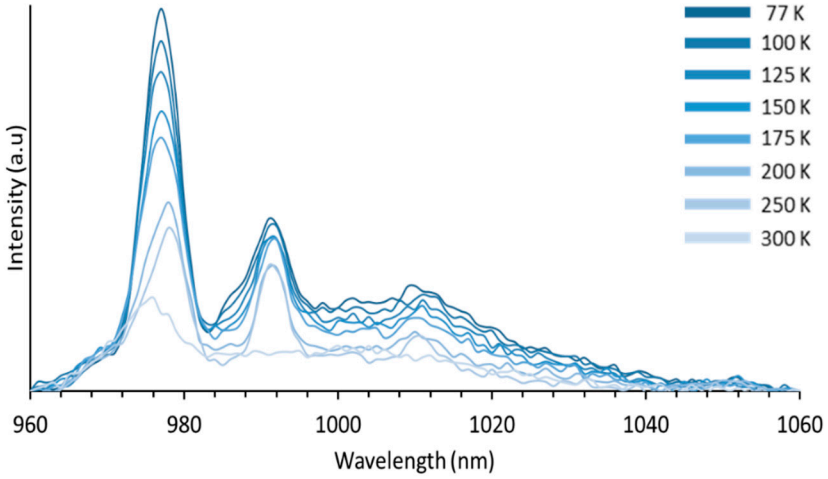

Figure 2. Dependence of the Yb emission intensity as a function of the temperature for a 5.3×10^{-5} M solution of YbL in D_2O containing 12% glycerol (λ_{exc} = 270 nm).

Table 1. Ytterbium lifetime in the range of 77–300 K (YbL = 5.3×10^{-5}, D_2O with 12% glycerol).

T **(°K)**	**77**	**100**	**125**	**150**	**175**	**200**	**250**	**273**	**300**
τ_{Yb} (µs)	14.4	14.1	14.7	14.7	14.5	13.3	11.0	11.1	9.9

3.4. Upconversion Experiments

In order to check the possibility of a Yb-to-Tb UC process, titration was performed in D_2O in which the Yb complex was titrated by additions of aliquots of a solution of $TbCl_3$ salts. The emission spectrum was recorded in the visible domain upon excitation at 980 nm in the $^2F_{5/2} \leftarrow {}^2F_{7/2}$ absorption band of Yb (Figure 3). After the first additions, characteristic Tb-centered emission bands emerged at 485, 545, 580 and 620 nm, corresponding to the $^5D_4 \rightarrow {}^7F_J$ (with J = 6, 5, 4 and 3, respectively) transitions of Tb. The signal then increased up to 1.5 eq and then formed a plateau right after. To confirm the UC process, a Log I vs. Log P plot was performed by monitoring the $^5D_4 \rightarrow {}^7F_5$ transition as a function of the power of the laser at 980 nm (Figure 4) for a mixture containing a 1.4 equivalent of Tb added to the Yb complex. A value close to 2 (1.92 found) indicated the involvement of two photons in the process and confirmed the UC phenomenon. The UC quantum yield was determined using a protocol described in the literature [6,11]. A value of 2.6×10^{-8} was obtained (P = 10.8 W cm^{-2}), which was of the same order of magnitude as those reported for similar compounds [11].

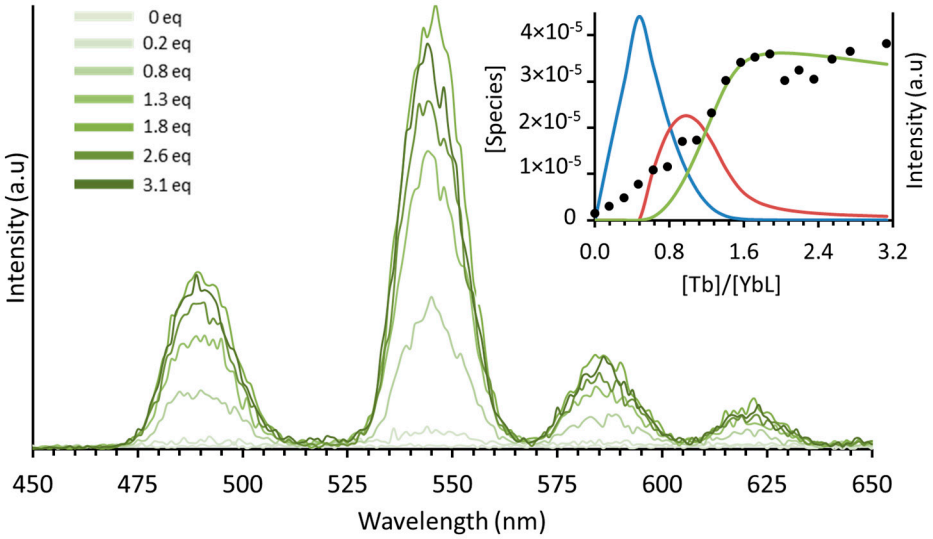

Figure 3. Evolution of the visible terbium emission during the titration of YbL by $TbCl_3 \cdot 6H_2O$ (λ_{ex} = 980 nm; YbL = 9.7 × 10^{-5} M; Tb = 7.7 × 10^{-4} M; solutions in D_2O, pD = 7.7). The inset shows the evolution of the UC intensity (black dots) and evolution of the concentrations of the species formed during the titration ($[(YbL)_2Tb]$, blue; $[(YbL)_2Tb_2]$, red and $[(YbL)_2Tb_3]$ in green).

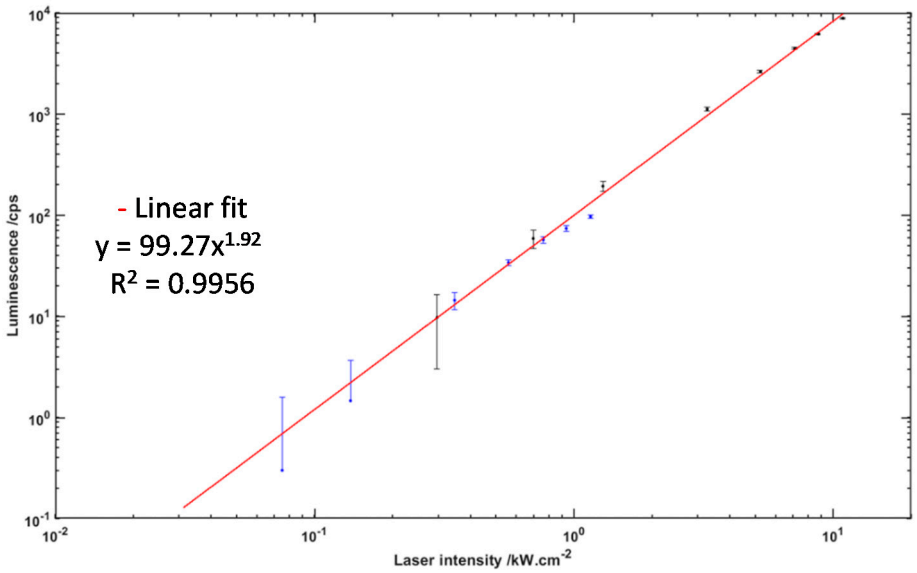

Figure 4. Log–log plot of the Tb-emitted intensity of the $^5D_4 \rightarrow {}^7F_5$ transition at 545 nm as a function of the excitation intensity of the 980 nm laser for a 5.3 × 10^{-5} M solution of YbL in D_2O containing a 1.4 equivalent of $TbCl_3 \cdot 6H_2O$.

The data of the titration were analyzed by a nonlinear least-squares method using Specfit software [40,41]. The analysis pointed to the formation of three emitting species, which were ascribed to $[(YbL)_2Tb_x]$ complexes with x = 1, 2 or 3. Their calculated distributions are presented in the inset of Figure 3. These compositions were consistent with previous spectroscopy titrations of the ligand by the addition of Ln(III) (Ln = Eu or Tb) [28]. All three species were able to generate UC, but the relative efficiencies, which were obtained thanks to the fitting procedure, pointed to the UC efficiencies of $[(YbL)_2Tb_2]$ and $[(YbL)_2Tb_3]$ being 1.84 and 5.6 times higher than that of $[(YbL)_2Tb]$, respectively.

To get deeper insight into the UC mechanism, time-resolved measurements were performed with a modulated 975-nm laser diode generating excitation pulses with a square temporal profile. As shown in Figure 5, 3–4 milliseconds were required for the rise of

the UC emission before the steady state was reached. This result indicated a slow kinetic step in the UC process which was related to the energy transfer occurring throughout the cooperative energy transfer UC process [27] (Scheme 2). The fit of the rising and decaying signals was made by using the model described by Nonat et al. [11] by updating the fitting data with the initial parameters (τ_{Yb} and ε_{Yb}). In this model, the presence of two species was assumed as a result of the presence of the different complexes in the solution. In our case, the addition of the 1.4 equivalent of Tb per Yb complex pointed to the presence of $[(YbL)_2Tb_2]$ and $[(YbL)_2Tb_3]$ as the dominant species in the solution. The upconversion lifetimes (i.e., the Tb luminescence lifetimes upon excitation at 980 nm) were determined to be 0.38 ± 0.04 ms and 1.86 ± 0.2 ms. The shorter Tb lifetime may be attributed to a Tb cation more exposed to the solvent molecules (with a higher hydration number). The associated UC rate constants k_{UC} were determined to be of 755 and 355 s^{-1}. In comparison with the literature, the UC rate constants obtained were somehow smaller but consistent with those reported in the literature [11,27,42].

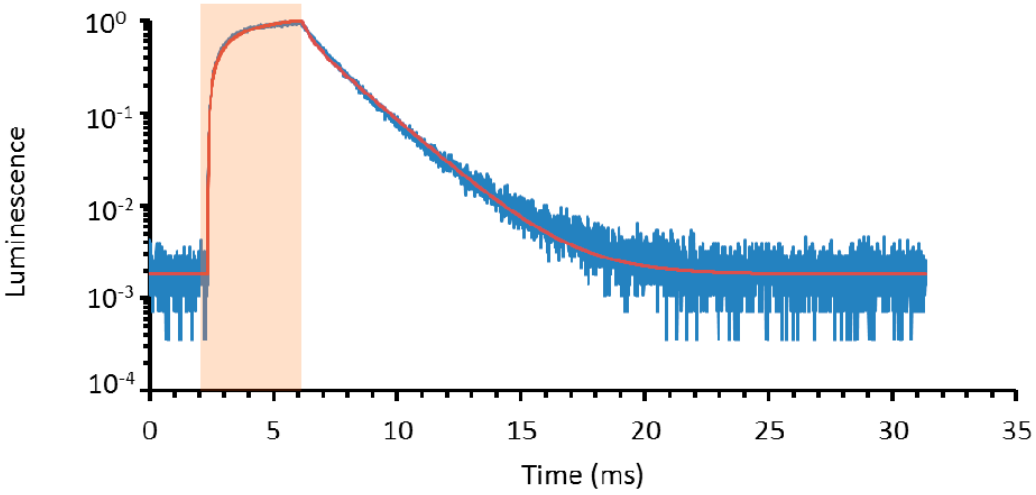

Figure 5. Time-resolved rise and decay curves of the Tb-centered UC emission intensity at 550 nm (in blue) upon time-gated excitation at 974 nm (8.1 kW cm^{-2}, orange square) for a 9.5 × 10^{-5} M solution of YbL in D_2O containing a 1.4 equivalent of $TbCl_3 \cdot 6H_2O$. The red line corresponds to the fit of the data (see text).

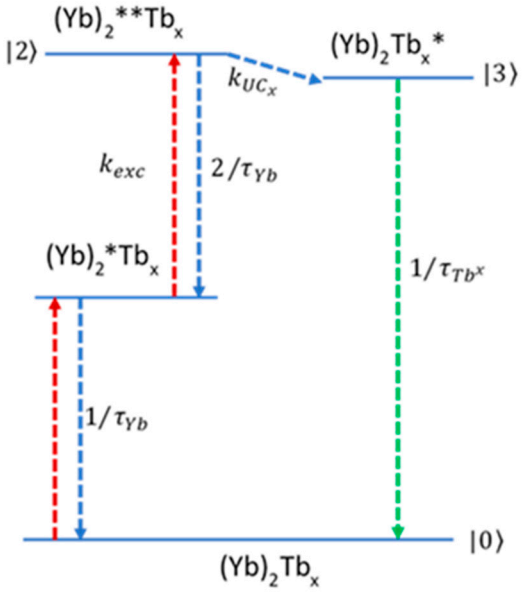

Scheme 2. Energy level diagram of the cooperative UC sensitization process in the $[(YbL)_2Tb_x]$ complex (x = 1–3). Symbols * and ** denote singly and doubly excited states respectively.

The energy transfer efficiency of the UC process η_{UC} was then calculated using Equation (4) [11]:

$$\eta_{UC} = \frac{\sum k_{UC}}{\sum k_{UC} + k_r + k_{nr}} \quad (4)$$

where k_{UC} represents the UC energy transfer rate. The radiative rate constant k_r of the Yb complex is the inverse of τ_r (1.13 ms) and is equal to 885 s^{-1}. The non-radiative rate constant k_{nr} is obtained from the intrinsic quantum yield Φ_{Yb}^{Yb} by

$$\Phi_{Yb}^{Yb} = \frac{k_r}{k_r + k_{nr}} \quad (5)$$

Using Φ_{Yb}^{Yb} = 1.5%, a value of 58,100 s^{-1} was obtained for k_{nr}. The energy transfer efficiency of the UC process η_{UC} was then calculated to be equal to 1.8%.

4. Conclusions

Our in-depth study of the YbL complex in D_2O showed a dependence on the hydration state as a function of the pD, resulting in the presence of two deuterated water molecules in the first coordination sphere of the complex at low pD values and a single one around the physiological pD. The dehydration was accompanied by a large increase in both the luminescence intensity and the excited state lifetime of the Yb emission. An increase in Yb emission was also observed at low temperatures as a result of decreased non-radiative transitions due to water molecules.

When the Yb complex was titrated by Tb^{3+} salts in a D_2O solution, heteropolynuclear $[(YbL)_2Tb_x]$ (x = 1–3) complexes formed, and direct excitation of the Yb atom at 980 nm in the heteronuclear complexes resulted in emission of the Tb atoms in the visible domain as a result of a cooperative sensitization UC mechanism. The energy transfer efficiency of the UC process was determined to be 1.8%, while the overall UC quantum yield value of 2.6×10^{-8} in D_2O was obtained for an excitation power density of 10.8 W cm^{-2}. Although weak, this value was in line with previous results in the literature [11], despite the presence of water molecules in the first coordination sphere of Yb. The improvement of the protection of Yb toward water de-excitation paves the way to even better UC devices for luminescence bioanalytical applications.

Author Contributions: Conceptualization, L.K.S. and C.C.; methodology, L.K.S., C.C. and L.J.C.; software, F.P.; validation, A.M.N. and L.J.C.; formal analysis, L.K.S. and F.P.; writing—original draft preparation, L.K.S. and L.J.C.; writing—review and editing, L.K.S., Y.M. and L.J.C.; supervision, L.J.C. All authors have read and agreed to the published version of the manuscript.

Funding: L.K.S. gratefully acknowledges the financial support from the French Ministère de l'enseignement supérieur et de la recherche and the France Canada Research Fund. C.C. and L.J.C. acknowledge the financial support of the French National Research Agency (project ANR LUCAS n° ANR-19-CE29-0014-01).

Institutional Review Board Statement: Not applicable.

Informed Consent Statement: Not applicable.

Data Availability Statement: On request to the authors.

Conflicts of Interest: The authors declare no competing financial interest.

References

1. Auzel, F. Upconversion and Anti-Stokes Processes with f and d Ions in Solids. *Chem. Rev.* **2004**, *104*, 139–173. [CrossRef]
2. Gamelin, D.R.; Güdel, H.U. Design of luminescent inorganic materials: New photophysical processes studied by optical spectroscopy. *Acc. Chem. Res.* **2000**, *33*, 235–242. [CrossRef]
3. Idris, N.M.; Jayakumar, M.K.G.; Bansal, A.; Zhang, Y. Upconversion nanoparticles as versatile light nanotransducers for photoactivation applications. *Chem. Soc. Rev.* **2015**, *44*, 1449–1478. [CrossRef]
4. Hemmer, E.; Benayas, A.; Légaré, F.; Vetrone, F. Exploiting the biological windows: Current perspectives on fluorescent bioprobes emitting above 1000 nm. *Nanoscale Horiz.* **2016**, *1*, 168–184. [CrossRef]

5. Zhu, X.; Su, Q.; Feng, W.; Li, F. Anti-Stokes shift luminescent materials for bio-applications. *Chem. Soc. Rev.* **2017**, *46*, 1025–1039. [CrossRef] [PubMed]
6. Chen, G.; Qiu, H.; Prasad, P.N.; Chen, X. Upconversion nanoparticles: Design, nanochemistry, and applications in Theranostics. *Chem. Rev.* **2014**, *114*, 5161–5214. [CrossRef]
7. Haase, M.; Schäfer, H. Upconverting Nanoparticles. *Angew. Chem. Int. Ed.* **2011**, *50*, 5808–5829. [CrossRef] [PubMed]
8. Suffren, Y.; Golesorkhi, B.; Zare, D.; Guénée, L.; Nozary, H.; Eliseeva, S.V.; Petoud, S.; Hauser, A.; Piguet, C. Taming Lanthanide-Centered Upconversion at the Molecular Level. *Inorg. Chem.* **2016**, *55*, 9964–9972. [CrossRef] [PubMed]
9. Nonat, A.; Chan, C.F.; Liu, T.; Platas-Iglesias, C.; Liu, Z.; Wong, W.-T.; Wong, W.-K.; Wong, K.-L.; Charbonnière, L.J. Room temperature molecular up conversion in solution. *Nat. Commun.* **2016**, *7*, 11978. [CrossRef]
10. Souri, N.; Tian, P.; Platas-Iglesias, C.; Wong, K.-L.L.; Nonat, A.; Charbonnière, L.J. Upconverted Photosensitization of Tb Visible Emission by NIR Yb Excitation in Discrete Supramolecular Heteropolynuclear Complexes. *J. Am. Chem. Soc.* **2017**, *139*, 1456–1459. [CrossRef] [PubMed]
11. Nonat, A.; Bahamyirou, S.; Lecointre, A.; Przybilla, F.; Mély, Y.; Platas-Iglesias, C.; Camerel, F.; Jeannin, O.; Charbonnière, L.J. Molecular Upconversion in Water in Heteropolynuclear Supramolecular Tb/Yb Assemblies. *J. Am. Chem. Soc.* **2019**, *141*, 1568–1576. [CrossRef]
12. Knighton, R.C.; Soro, L.K.; Lecointre, A.; Pilet, G.; Fateeva, A.; Pontille, L.; Francés-Soriano, L.; Hildebrandt, N.; Charbonnière, L.J. Upconversion in molecular hetero-nonanuclear lanthanide complexes in solution. *Chem. Commun.* **2021**, *57*, 53–56. [CrossRef]
13. Bünzli, J.C.G.; Piguet, C. Taking advantage of luminescent lanthanide ions. *Chem. Soc. Rev.* **2005**, *34*, 1048–1077. [CrossRef] [PubMed]
14. Bünzli, J.C.G. On the design of highly luminescent lanthanide complexes. *Coord. Chem. Rev.* **2015**, *293–294*, 19–47. [CrossRef]
15. Gnach, A.; Lipinski, T.; Bednarkiewicz, A.; Rybka, J.; Capobianco, J.A. Upconverting nanoparticles: Assessing the toxicity. *Chem. Soc. Rev.* **2015**, *44*, 1561–1584. [CrossRef] [PubMed]
16. Horrocks, W.D., Jr.; Sudnick, D.R. Lanthanide Ion Probes of Structure in Biology. Laser-Induced Luminescence Decay Constants Provide a Direct Measure of the Number of Metal-Coordinated Water Molecules. *J. Am. Chem. Soc.* **1979**, *101*, 334–340. [CrossRef]
17. Beeby, A.; Clarkson, I.M.; Dickins, R.S.; Faulkner, S.; Parker, D.; Royle, L.; de Sousa, A.S.; Williams, J.A.G.; Woods, M. Non-radiative deactivation of the excited states of europium, terbium and ytterbium complexes by proximate energy-matched OH, NH and CH oscillators: An improved luminescence method for establishing solution hydration states. *J. Chem. Soc. Perkin Trans.* **1999**, *2*, 493–504. [CrossRef]
18. Bischof, C.; Wahsner, J.; Scholten, J.; Trosien, S.; Seitz, M. Quantification of C-H quenching in near-IR luminescent ytterbium and neodymium cryptates. *J. Am. Chem. Soc.* **2010**, *132*, 14334–14335. [CrossRef] [PubMed]
19. Charbonnière, L.; Mameri, S.; Kadjane, P.; Platas-Iglesias, C.; Ziessel, R. Tuning the coordination sphere around highly luminescent lanthanide complexes. *Inorg. Chem.* **2008**, *47*, 3748–3762. [CrossRef]
20. Zhang, T.; Zhu, X.; Cheng, C.C.W.; Kwok, W.M.; Tam, H.L.; Hao, J.; Kwong, D.W.J.; Wong, W.K.; Wong, K.L. Water-soluble mitochondria-specific ytterbium complex with impressive NIR emission. *J. Am. Chem. Soc.* **2011**, *133*, 20120–20122. [CrossRef]
21. Nonat, A.M.; Charbonnière, L.J. Upconversion of light with molecular and supramolecular lanthanide complexes. *Coord. Chem. Rev.* **2020**, *409*, 213192. [CrossRef]
22. Zare, D.; Suffren, Y.; Guénée, L.; Eliseeva, S.V.; Nozary, H.; Aboshyan-Sorgho, L.; Petoud, S.; Hauser, A.; Piguet, C. Smaller than a nanoparticle with the design of discrete polynuclear molecular complexes displaying near-infrared to visible upconversion. *Dalton Trans.* **2015**, *44*, 2529–2540. [CrossRef] [PubMed]
23. Hemmer, E.; Venkatachalam, N.; Hyodo, H.; Hattori, A.; Ebina, Y.; Kishimoto, H.; Soga, K. Upconverting and NIR emitting rare earth based nanostructures for NIR-bioimaging. *Nanoscale* **2013**, *5*, 11339–11361. [CrossRef]
24. Meijer, M.S.; Rojas-Gutierrez, P.A.; Busko, D.; Howard, I.A.; Frenzel, F.; Würth, C.; Resch-Genger, U.; Richards, B.S.; Turshatov, A.; Capobianco, J.A.; et al. Absolute upconversion quantum yields of blue-emitting $LiYF_4$:Yb^{3+},Tm^{3+} upconverting nanoparticles. *Phys. Chem. Chem. Phys.* **2018**, *20*, 22556–22562. [CrossRef]
25. Zhou, B.; Yan, L.; Tao, L.; Song, N.; Wu, M.; Wang, T.; Zhang, Q. Enabling Photon Upconversion and Precise Control of Donor–Acceptor Interaction through Interfacial Energy Transfer. *Adv. Sci.* **2018**, *5*, 1700667. [CrossRef]
26. Salley, G.M.; Valiente, R.; Guedel, H.U. Luminescence upconversion mechanisms in Yb^{3+}–Tb^{3+} systems. *J. Lumin.* **2001**, *94–95*, 305–309. [CrossRef]
27. Salley, G.M.; Valiente, R.; Güdel, H.U. Phonon-assisted cooperative sensitization of Tb^{3+} in $SrCl_2$:Yb, Tb. *J. Phys. Condens. Matter* **2002**, *14*, 301. [CrossRef]
28. Charpentier, C.; Salaam, J.; Lecointre, A.; Jeannin, O.; Nonat, A.; Charbonnière, L.J. Phosphonated Podand Type Ligand for the Complexation of Lanthanide CationsPhosphonated Podand Type Ligand for the Complexation of Lanthanide Cations. *Eur. J. Inorg. Chem.* **2019**, *2019*, 2168–2174. [CrossRef]
29. Mikkelsen, K.; Siguri, A.; Nielsen, O. Acidity measurements jyith the glass electrode is h,o-d,o mixtures. *J. Phys. Chem.* **1960**, *64*, 632–637. [CrossRef]
30. Weibel, N.; Charbonnière, L.J.; Guardigli, M.; Roda, A.; Ziessel, R. Engineering of Highly Luminescent Lanthanide Tags Suitable for Protein Labeling and Time-Resolved Luminescence Imaging. *J. Am. Chem. Soc.* **2004**, *126*, 4888–4896. [CrossRef]

31. Charpentier, C.; Salaam, J.; Nonat, A.; Carniato, F.; Jeannin, O.; Brandariz, I.; Esteban-Gomez, D.; Platas-Iglesias, C.; Charbonnière, L.J.; Botta, M. pH-Dependent Hydration Change in a Gd-Based MRI Contrast Agent with a Phosphonated Ligand. *Chem.-A Eur. J.* **2020**, *26*, 5407–5418. [CrossRef]
32. Ziessel, R.F.; Ulrich, G.; Charbonnière, L.; Imbert, D.; Scopelliti, R.; Bünzli, J.C.G. NIR lanthanide luminescence by energy transfer from appended terpyridine-boradiazaindacene dyes. *Chem.-A Eur. J.* **2006**, *12*, 5060–5067. [CrossRef]
33. Asano-Someda, M.; Kaizu, Y. Hot bands of (f, f*) emission from ytterbium(III) porphyrins in solution. *J. Photochem. Photobiol. A Chem.* **2001**, *139*, 161–165. [CrossRef]
34. Shavaleev, N.M.; Scopelliti, R.; Gumy, F.; Bünzli, J.C.G. Surprisingly bright near-infrared luminescence and short radiative lifetimes of ytterbium in hetero-binuclear Yb-Na chelates. *Inorg. Chem.* **2009**, *48*, 7937–7946. [CrossRef]
35. Werts, M.H.V.; Jukes, R.T.F.; Verhoeven, J.W. The emission spectrum and the radiative lifetime of Eu^{3+} in luminescent lanthanide complexes. *Phys. Chem. Chem. Phys.* **2002**, *4*, 1542–1548. [CrossRef]
36. Eliseeva, S.V.; Bünzli, J.C.G. Lanthanide luminescence for functional materials and bio-sciences. *Chem. Soc. Rev.* **2010**, *39*, 189–227. [CrossRef]
37. Bünzli, J.C.G. Lanthanide luminescence for biomedical analyses and imaging. *Chem. Rev.* **2010**, *110*, 2729–2755. [CrossRef]
38. Nocton, G.; Nonat, A.; Gateau, C.; Mazzanti, M. Water stability and luminescence of lanthanide complexes of tripodal ligands derived from 1,4,7-triazacyclononane: Pyridinecarboxamide versus pyridinecarboxylate donors. *Helv. Chim. Acta* **2009**, *92*, 2257–2273. [CrossRef]
39. Knighton, R.C.; Soro, L.K.; Troadec, T.; Mazan, V.; Nonat, A.M.; Elhabiri, M.; Saffon-Merceron, N.; Djenad, S.; Tripier, R.; Charbonnière, L.J. Formation of Heteropolynuclear Lanthanide Complexes Using Macrocyclic Phosphonated Cyclam-Based Ligands. *Inorg. Chem.* **2020**, *59*, 10311–10327. [CrossRef] [PubMed]
40. Gampp, H.; Maeder, M.; Meyer, C.J.; Zuberbühler, A.D. Calculation of equilibrium constants from multiwavelength spectroscopic data-III. Model-free analysis of spectrophotometric and ESR titrations. *Talanta* **1985**, *32*, 1133–1139. [CrossRef] [PubMed]
41. Maeder, M.; Zuberbühler, A.D. Nonlinear Least-Squares Fitting of Multivariate Absorption Data. *Anal. Chem.* **1990**, *62*, 2220–2224. [CrossRef]
42. Suffren, Y.; Zare, D.; Eliseeva, S.V.; Guénée, L.; Nozary, H.; Lathion, T.; Aboshyan-Sorgho, L.; Petoud, S.; Hauser, A.; Piguet, C. Near-Infrared to Visible Light-Upconversion in Molecules: From Dream to Reality. *J. Phys. Chem. C* **2013**, *117*, 26957–26963. [CrossRef]